DOI: 10.1002/chem.200601376

Tuning the Excited-State Energy of the Organic Chromophore in Bichromophoric Systems Based on the Ru^{II} Complexes of Tridentate Ligands

Elaine A. Medlycott,[a] Garry S. Hanan,*[a] Frédérique Loiseau,[b] and Sebastiano Campagna*[b]

Abstract: A series of new heteroleptic and homoleptic Ru^{II} complexes containing variously substituted bis(pyridyl)triazine ligands has been prepared and their absorption spectra, redox behaviour and luminescence properties (both in fluid solution at room temperature and in a rigid matrix at 77 K) have been investigated. For some compounds, X-ray structures have also been determined. The new bis(pyridyl)triazines incorporate additional chromophores, such as biphenyl, phenanthrene, anthracene and bromoanthracene derivatives, so the Ru^{II} species can be considered as multichromophoric species. The absorption spectra and redox properties of all the metal complexes have been assigned to features belonging to specific subunits, thus suggesting that these species can be regarded as multicomponent, supramolecular assemblies from an electronic coupling point of view. Whereas most of the complexes exhibit luminescence properties that can be attributed to metal-to-ligand charge-transfer (MLCT) states involving the metal-based subunit(s), the species containing the anthryl and, even more, the brominated anthryl chromophores exhibit complicated luminescence behaviour. For example, **2d** (the anthryl-containing heteroleptic metal compound) exhibits MLCT emission at room temperature and emission from the anthracene triplet at 77 K; **2e** (the bromo-substituted anthryl-containing heteroleptic metal compound) exhibits anthryl-based emission at 77 K and MLCT emission at room temperature, but with a prolonged lifetime, thus suggesting equilibration between two triplet states that belong to different chromophores. The equilibration regime between MLCT and aromatic hydrocarbon triplet states is therefore reached by suitable substitution on the organic chromophore.

Keywords: cyclic voltammetry · emission spectroscopy · multichromophoric effect · ruthenium · triazine ligands

Introduction

Ru^{II} complexes of polypyridine ligands have been intensely researched as a result of their excellent photophysical properties and promising applications as photoactive devices.[1,2] The most studied complexes are based on $[Ru(bpy)_3]^{2+}$ (bpy = 2,2′-bipyridine), as they have been shown to have long-lived excited states at room temperature that originate from their metal-to-ligand charge-transfer (MLCT) state.[3–5] However, bpy-based complexes induce chirality at the metal centre, and separation of the diastereomers in polymetallic complexes, although possible,[6] can be complicated, thus attention has been turned to achiral tridentate 2,2′:6′,2″-terpyridine (tpy)-type ligands.[7] Although tpy is a synthetically appealing target, on coordination to the metal ion, the tridentate ligand imposes a small bite angle and consequently its ligand-field strength is lower than that of bpy.[8] This behaviour allows thermal access to low-lying non-emissive metal-centred (MC) states, and the MLCT excited-state is short lived (0.25 ns for $[Ru(tpy)_2]^{2+}$).[9] Many strategies have been used to prolong excited-state lifetimes of complexes with tridentate ligands, with most focusing on the manipulation of the energies of non-emissive MC states relative to emissive MLCT states.[10,11] One such strategy makes use of electron-

[a] E. A. Medlycott, Prof. Dr. G. S. Hanan
Département de Chimie
Université de Montréal
2900 Edouard Montpetit, Montréal, QC, H3T 1J4 (Canada)
Fax: (+1) 514-343-2468
E-mail: garry.hanan@umontreal.ca

[b] Dr. F. Loiseau, Prof. Dr. S. Campagna
Dipartimento di Chimica Inorganica
Chimica Analitica e Chimica Fisica, Università di Messina
Via Sperone 31, 98166 Messina (Italy)
Fax: (+39) 090-393-756
E-mail: campagna@unime.it

Supporting information for this article is available on the WWW under http://www.chemeurj.org/ or from the author.

deficient triazine ligands, which function to lower the energy of the ^{3}MLCT state relative to the metal-centred state (Scheme 1).[12,13] For this type of complex, excited-state lifetimes were extended to 8 ns at room temperature, thirty-times greater than that of the parent complex.

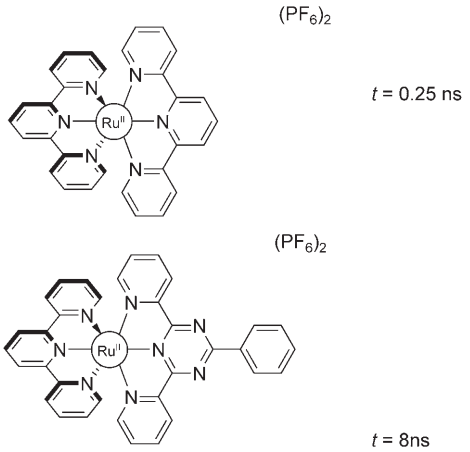

Scheme 1. Heteroleptic complex that incorporates a central triazine ring relative to the parent complex $[Ru(tpy)_2]^{2+}$.[13]

An alternative strategy has made use of the "multichromophoric approach",[14] which relies on the presence of additional chromophore(s) with a non-emissive, long-lived triplet state of comparable energy to the ^{3}MLCT state.[14,15] Reversible population of the triplet excited state localised on the additional chromophore(s) can occur, thereby delaying emission from the complex and prolonging the MLCT excited-state lifetime, with the organic triplet behaving as an excited-state storage element for MLCT emission. Initially, this approach was used for Ru^{II} complexes of bidentate bipyridine-type ligands[15] and was later applied to tridentate tpy-type systems as well.[16,17] Usually, the organic chromophore triplet is lower in energy than the triplet MLCT level, however, in rare examples the reverse is obtained,[17] although this makes the multichromophoric effect less efficient.

In all the multichromophoric species investigated so far, it is the MLCT state energy that has been modified, by polypyridine ligand substitution or selection, to fit the suitable organic chromophore triplet energy. Herein, we exploit the possibility of using substituents on the organic chromophore to activate the multichromophoric behaviour. As suitable systems, we selected a family of Ru^{II} triazine-based complexes coupled with variously substituted anthracene or phenanthrene subunits. In such cases, the Ru-to-triazine CT level can be lower in energy than either the phenanthrene or anthracene triplets, so that the multichromophoric behaviour is not active in the simplest compounds. However, introduction of the bromo substituent on anthracene lowers the energy of the anthracene components and the multichromophoric behaviour can take place. Therefore, the systems investigated herein belong to the much less explored case in which the MLCT level is the lowest-energy state of the two states involved in the equilibration process.[18]

The structural formulae for the studied compounds are shown in Scheme 2. A bromo substituent in the 4-position of the pendant phenyl ring allows a "chemistry-on-the-complex" approach to introduce additional organic components with varying triplet-state energies.[16,19–23]

Results and Discussion

Synthesis: Two approaches were applied to the synthesis of complexes **2a–e** and **3a–e**. We previously reported a classical synthetic procedure for the preparation of **3c**, the "ligand-synthesis" approach, in which the phenanthryl group was introduced onto the triazine ligand prior to complexation.[31] Alternatively, the brominated ligand **L1** can be coordinated to the Ru^{II} centre, thus affording an ideal precursor for the "chemistry-on-the-complex" approach and enabling the introduction of organic components using cross-coupling reactions.[16,19,20,23,32–35]

To evaluate the effectiveness of the "chemistry-on-the-complex" approach, we set out to synthesise complexes **2b–e** and **3b–e** in this fashion (Scheme 3). Thus, complex **2a** was synthesised by the addition of **L1**, prepared according to a previously reported procedure,[27] to a suspension of one equivalent of $[RuCl_3(tpy)]$[28] and three equivalents of $AgNO_3$ in ethanol. After heating at reflux for four hours, the resulting dark solution was cooled, filtered to remove AgCl and dried under reduced pressure. The residue was solubilised and a precipitate formed on addition to aqueous NH_4PF_6. The precipitate was collected and purified by column chromatography using acetonitrile/KNO_3(saturated) (7:1) as the eluent. The second intense red band was collected and was precipitated as its PF_6^- salt.

It was found that a one-pot synthesis of **3a** was more successful than the two-step approach, which would involve the formation of a $[RuCl_3(\mathbf{L1})]$ intermediate. Two equivalents of the ligand were added to one equivalent of $[RuCl_3]\cdot 3H_2O$ and three equivalents of $AgNO_3$ in *N*,*N*-dimethylformamide (DMF). The reaction mixture was stirred in DMF at room temperature for 20 min, heated to reflux for 1 h, cooled and purified as for **2a**. Complexes **2b–d** and **3b–d** were synthesised by using the palladium-catalysed Suzuki–Miyaura reaction in degassed DMF by adapting known procedures (Scheme 3).[16,29] The complexes could be worked up by precipitation in aqueous NH_4PF_6 and then isolated by column chromatography on silica gel with MeCN/KNO_3(saturated) (9:1) as the eluant. Counterion exchange to form the PF_6 salts afforded **2b–d** and **3b–d**.

The synthesis of **2e** was attempted by using the "chemistry-on-the-complex" approach; however, the reaction proceeded slowly and the purification of **2e** was difficult. An alternative approach introduced the bromoanthracene substituent into the ligand prior to complexation in a similar manner to the approach previously employed for the synthesis of **3c**.[31] A Suzuki–Miyaura reaction afforded *p*-(10-bro-

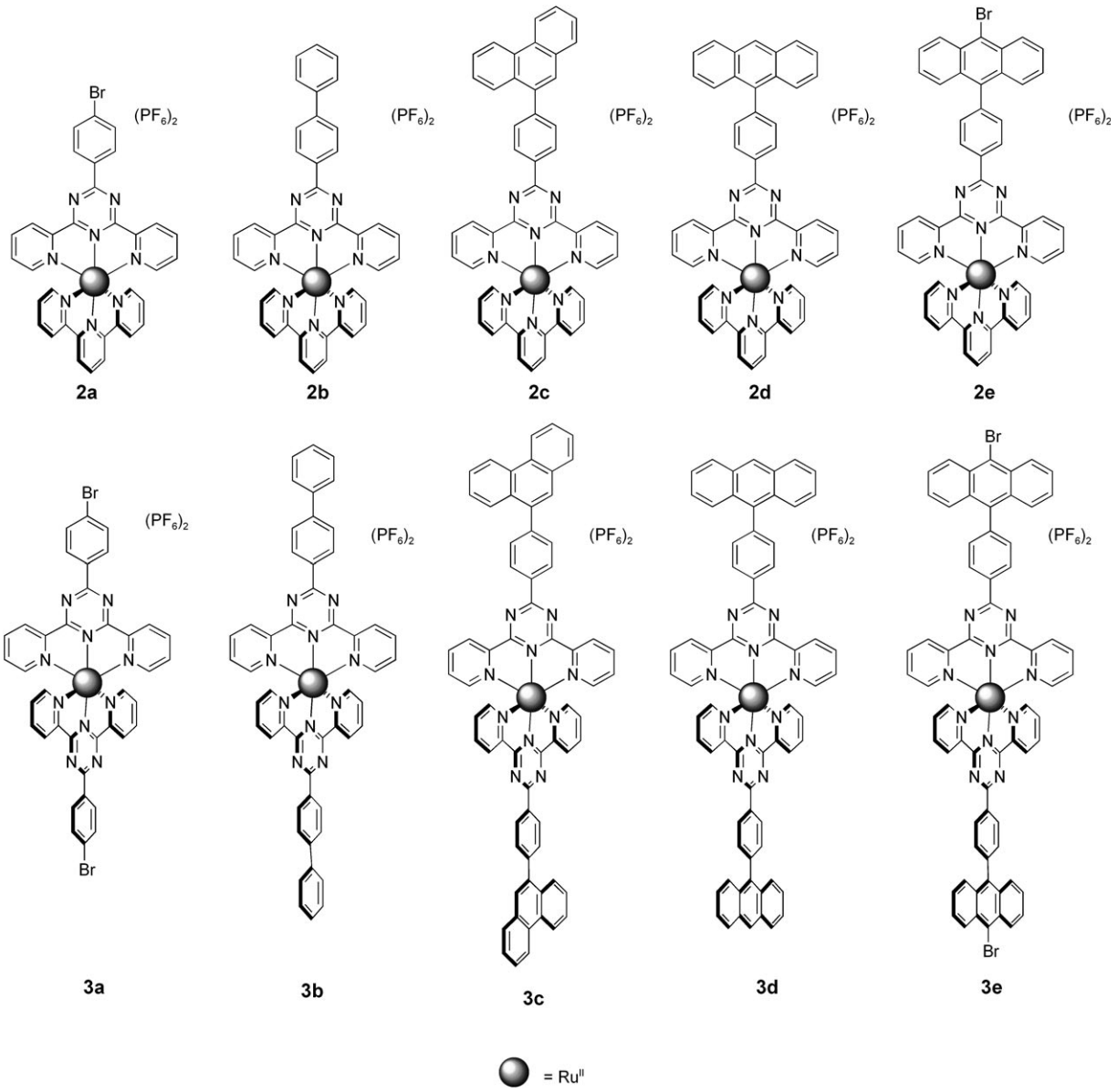

Scheme 2. Heteroleptic complexes **2a–e** and homoleptic complexes **3a–e**.

moanthryl)benzonitrile, thus modifying a previously reported procedure to monosubstitute 9,10-dibromoanthracene using 4-cyanophenylboronic acid.[30,36] *p*-(10-Bromoanthryl)-benzonitrile could then be used to synthesise the triazine ligand by employing the same procedure as used for **L1**.[27,31]

The ^{1}H NMR spectra for **3d** and **3e** in CD_3CN at 400 MHz are shown in Figure 1. The bromo substituent has little effect on the chemical shift of the pyridyl protons (labelled in Figure 1), but the signals for the anthracene-based protons in **3e** are significantly deshielded with respect to those in **3d.** The disappearance of the anthracene-based singlet at the 10-position probes the bromo substitution of the anthracene moiety.

X-ray crystallography: The solid-state structures of **L2** and complexes **2a**, **2b** and **3a** were studied by X-ray diffraction (Table 1 and Figures 2 and 3). Y-ray quality crystals of **L2** were obtained by slow diffusion of hexane into a concentrated solution of **L2** in $CHCl_3$.

The ligand crystallises in the orthorhombic space group $P2_12_12_1$ with four molecules in the unit cell. The two pyridyl and phenyl rings twist away from the triazine ring by 15.6(2), 14.7(2) and 7.0(2)°, respectively. The pyridyl rings are twisted twice as much as the phenyl ring as a result of a combination of π-stacking effects between neighbouring molecules and the N–N lone-pair repulsions between the pyridyl N atoms and triazine-based N atoms. The ligand molecules aggregate through continuous π-stacking interactions in the extended lattice between the anthryl tail of one

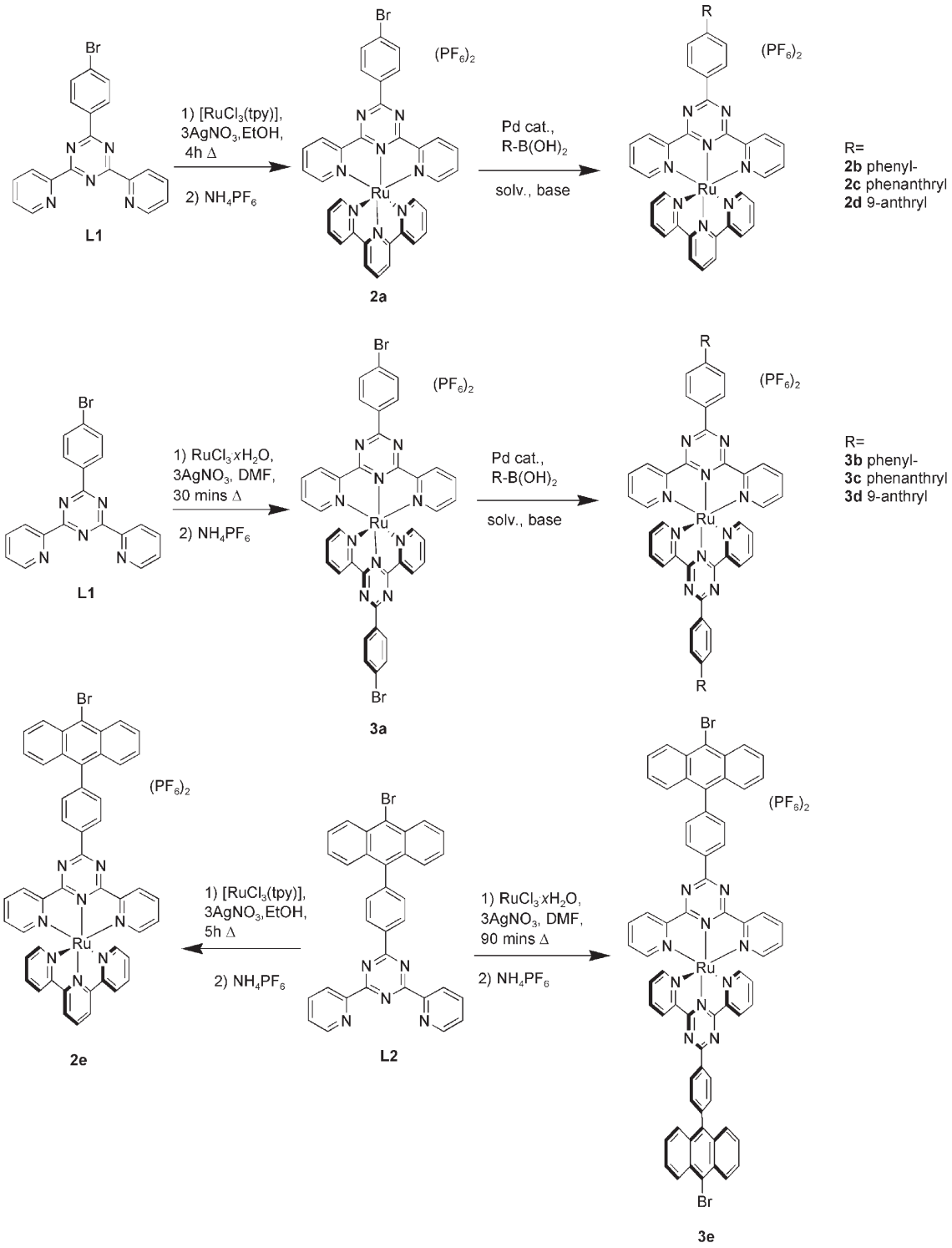

Scheme 3. Synthesis of complexes **2a–e** and **3a–e**. solv. = solvent.

molecule and the pyridyl head of the neighbouring molecule (Figure 2). The centroid–centroid distances between the central anthryl ring and the pyridyl rings above and below the plane are 3.30 and 4.48 Å, respectively.

Crystals of **2a** and **3a** were obtained by slow diffusion of isopropyl ether into a concentrated solution of the complexes in acetonitrile. Complex **2a** crystallised in the triclinic space group $P\bar{1}$ with two cations, four PF_6^- ions and four molecules of acetonitrile in the asymmetric unit. The pendant phenyl rings are twisted by 7.6(2) and 9.5(2)° for both independent cations (Table 1). The near coplanar configurations are due to intramolecular hydrogen-bonding interac-

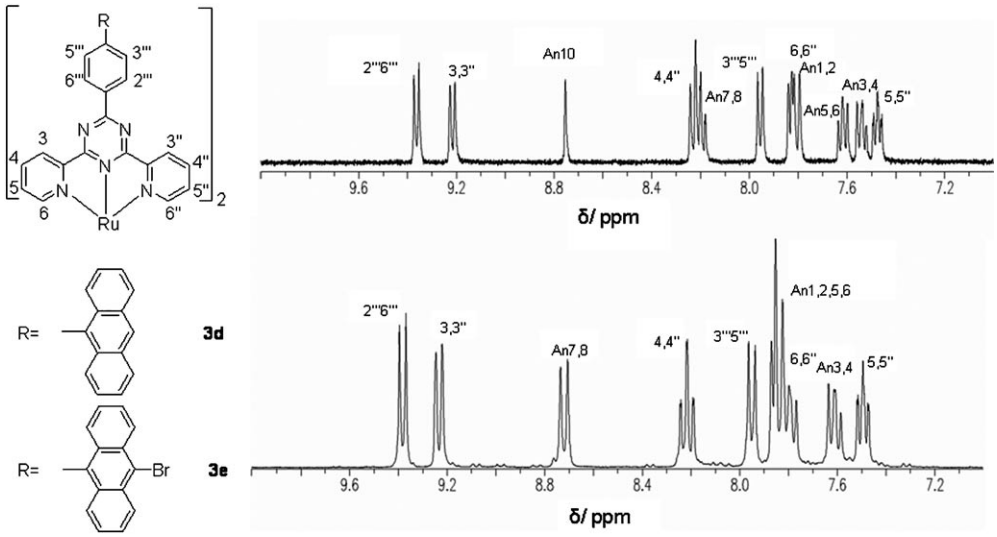

Figure 1. ^{1}H NMR spectra of complexes **3d** (top) and **3e** (bottom) at 400 MHz in CD_3CN.

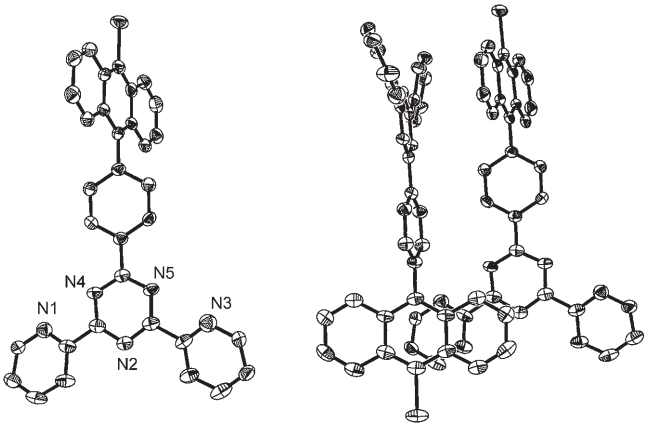

Figure 2. X-ray crystal structure of **L2** (left) as an ORTEP representation. Thermal ellipsoids are set at the 50% probability level. The π-stacking, face-to-face interactions are shown (right).

tions between the lone pairs on the triazine atoms N4 and N5 and the C–H bond on the phenyl substituent. The slight twist is imposed by edge-to-face interactions of the phenyl ring with the pyridyl ring of a neighbouring cation (H···centroid: 2.86 and 3.19 Å).

The Ru–N bond lengths and N-Ru-N bond angles are reported in Table 1. Longer Ru–N bond lengths to the pyridyl rings for both the triazine and tpy ligands are observed and are a result of the constrained bite angle imposed by the terdentate ligands.[37] The Ru–N(trz) central bond (M–N2/N10) is shorter than the Ru–N7(tpy) bond (M–N7/N15). This finding is consistent with that previously reported for triazine-based complexes and is presumably a result of the improved π-acceptor properties of the electron-deficient triazine ligand.[13] The Ru–N(tpy) bond lengths are consistent with those previously reported for $[Ru(tpy)_2]^{2+}$.[38]

It can be noted that the tridentate bite angles N-M-N in the triazine-based ligands are smaller (155.5–155.6°) than those in the tpy-based ligands (157.4–158.2°). The additional N atoms in the triazine ring distort the ring angles away from the ideal 120° in benzene significantly more than in the central pyridyl ring of tpy. This behaviour will have a negative effect on the ligand-field strength, thereby facilitating thermal access of metal-centred states (see below).

Complex **3a** crystallises in the monoclinic space group *C2/c* and is isostructural to the reported Fe^{II}, Co^{II} and Cu^{II} complexes of **L1**.[27,39] Short bromine–bromine contacts are observed in the solid state, and these interactions are smaller than the sum of the Van der Waals radii (3.48 Å). In the absence of stabilizing π-stacking interactions, these contacts influence the cationic arrangements in the extended lattice.

Efforts to obtain crystals of **2b** as the PF_6^- salt were unsuccessful under a variety of solvent conditions. However, the addition of an excess of ammonium tetraphenylborate to a solution of **2b** in acetonitrile allowed salt exchange, and the complex was crystallised as a mixed salt containing one PF_6^- and one BPh_4^- ion per cation. The Ru–N bond lengths and N-Ru-N bond angles are very similar to those of **2a**, thus indicating that the substitution on the periphery has little effect on the metal centre. The phenyl ring closest to the triazine ring is twisted by 4.6(2)° in a near coplanar interaction. The second phenyl ring is twisted by 26.4(2)° about the linking C–C bond, which is consistent with the twist reported for Ru^{II} complexes of biphenyl–tpy-type systems.[37] Edge-to-face interactions between the biphenyl tails promote the twists about the interannular C–C bond. The inner phenyl-ring face has a short contact with the outer phenyl-ring edge of a neighbouring cation (H···centroid: 2.71 Å). An additional edge-to-face interaction is observed with a short contact of the face of the outer phenyl ring with a neighbouring pyridyl ring (H···centroid: 3.10 Å).

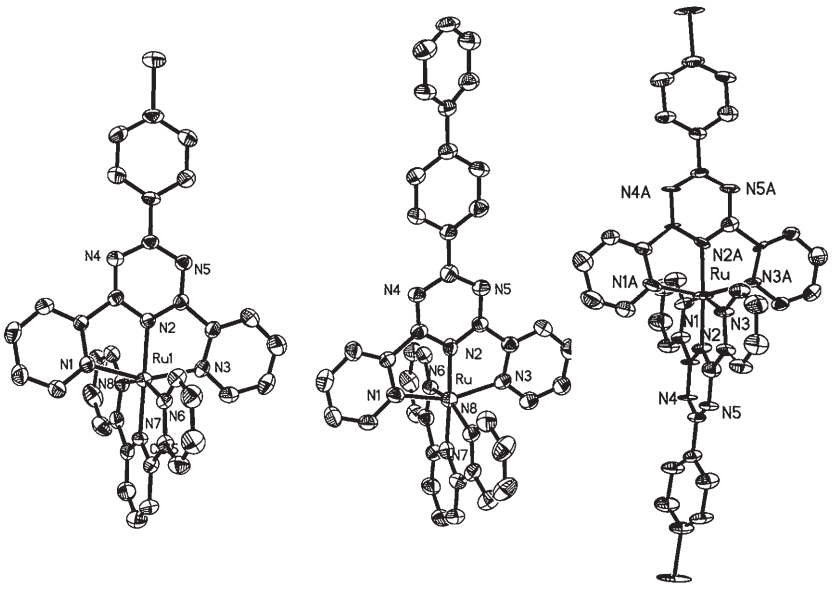

Figure 3. X-ray crystal structure of **2a** (left)**, 2b** (central) and **3a** (right) as ORTEP representations. Thermal ellipsoids are set at the 50% probability level. The anions and H atoms have been omitted for clarity.

Table 1. Selected bond lengths and angles from the X-ray structural analysis of **2a**, **2b** and **3a**.

	2a		**2b**	**3a**	$[Ru(tpy)_2]^{2+}$ [a]
bond lengths [Å]					
M−N1	2.089 (4)	2.106 (4)	2.084 (4)	2.096 (5)	2.07 (1)
M−N2(trz)	1.957 (4)	1.966 (4)	1.955 (3)	1.972 (5)	1.99 (1)
M−N3	2.101 (4)	2.083 (4)	2.081 (4)	2.085 (5)	2.05 (1)
M−N6	2.065 (4)	2.081 (4)	2.084 (4)		2.09 (1)
M−N7	1.986 (4)	1.985 (4)	1.985 (3)		1.96 (1)
M−N8	2.075 (4)	2.067 (4)	2.054 (4)		2.07 (1)
bond angles [°]					
N1-M-N3	155.60 (15)[b]	155.7 (2)[b]	155.60 (16)[b]	155.45 (19)	158.1 (4)
N6-M-N8	157.34 (16)[c]	157.6 (2)[c]	158.08 (16)[c]		158.2 (4)
trz–phenyl twist	7.60 (24)	9.47 (24)	4.60 (22)	14.71 (47)	
phenyl–phenyl twist			26.35 (24)		

[a] Data from reference [38]. [b] N-M-N tridentate bite angle for the triazine ligand. [c] N-M-N tridentate bite angle for the tpy ligand.

Electrochemistry: Cyclic voltammetric studies of the complexes were performed (Table 2). As can be seen by the difference between the cathodic and anodic peak potentials in Table 2, none of the processes are truly reversible, a fact confirmed in most cases by the I_c/I_a ratios.[41] Complexes **2a–c** and **2e** all have a single one-electron oxidation assigned to the Ru^{III}/Ru^{II} couple as noted for similar complexes.[13] Complex **2d** has two oxidative processes, the first is assigned to an anthracene-based oxidation and the second to a Ru^{III}/Ru^{II} couple (Figure 4). The irreversibility of both processes is confirmed by the difference between the cathodic and anodic peak potentials and the I_c/I_a ratios. The Ru^{III}/Ru^{II} couple is at approximately the same potential as in the other complexes, thus indicating that the anthracene component is electronically separated from the Ru^{II} metal centre. Introduction of the bromo substituent significantly affects the oxidation potential of the anthracene moiety. The first irreversible oxidation of **2e** corresponds to the Ru^{III}/Ru^{II} couple, and no subsequent anthracene oxidations are observed up to +2.0 V.

All the heteroleptic complexes **2a–e** have three one-electron reductions, which are assignable by comparison with previously reported results.[13] The first reduction is triazine-based and is observed at a less negative potential than in

Table 2. Half-wave potentials for **2a–d** and **3a–d**.[a]

	$E_{1/2}$ (ox.)		$E_{1/2}$ (red.)			
2a	1.43 (79, 0.9)		−0.75 (64, 1.1)	−1.37 (68, 1.0)	−1.62 (107, 0.7)	
2b	1.40 (71, 0.9)		−0.78 (53, 1.3)	−1.39 (66, 1.1)	−1.65 (82, 1.0)	
2c	1.45 (80, 1.1)		−0.81 (82, 0.9)	−1.45 (90, 0.8)	−1.71 (90, 0.9)	
2d	1.29 (64, 1.2)	1.43 (98, 0.9)	−0.77 (48, 1.8)	−1.39 (62, 1.0)	−1.64 (70, 1.6)	
2e	1.43 (91, 0.8)		−0.77 (74, 1.2)	−1.40 (79, 1.2)	−1.66 (80, 1.1)	
3a	1.53 (76, 0.6)		−0.71 (50, 1.2)	−0.87 (55, 1.3)	−1.51 (70, 1.2)	−1.71 (128, 0.7)
3b	1.53 (82, 1.0)		−0.78 (84, 0.8)	−0.97 (50, 0.7)	−1.58 (50, 0.9)	−1.79 (138, 1.2)
3c[b]	1.53 (70, 1.1)		−0.73 (53, 1.0)	−0.89 (45, 1.0)	−1.55 (77, 1.2)	−1.78 (72, 1.1)
3d	1.32 (42, 0.9)	1.61 (173, 1.1)	−0.74 (48, 0.9)	−0.91 (50, 1.2)	−1.55 (64, 1.0)	−1.80 (61, 0.9)
3e	1.38 (80, 1.2)	1.57 (87, 1.2)	−0.71 (82, 0.9)	−0.86 (73, 1.2)	−1.43 (irr, 0.06)	
$[Ru(tpy)_2]^{2+}$ [c]	1.31 (60)		−1.23 (70)	−1.47 (69)		

[a] Potentials are given in volts and are versus the saturated calomel electrode (SCE) for solutions in acetonitrile, 0.1 M in tetra-*n*-butylammonium hexafluorophosphate (TBAP), recorded at 25±1°C at a sweep rate of 200 $mV s^{-1}$; the difference between the cathodic and anodic peak potentials (millivolts) and I_c/I_a ratios are given in parentheses. ox. = oxidation, red. = reduction. [b] Data from reference [31]. [c] Data from reference [40].

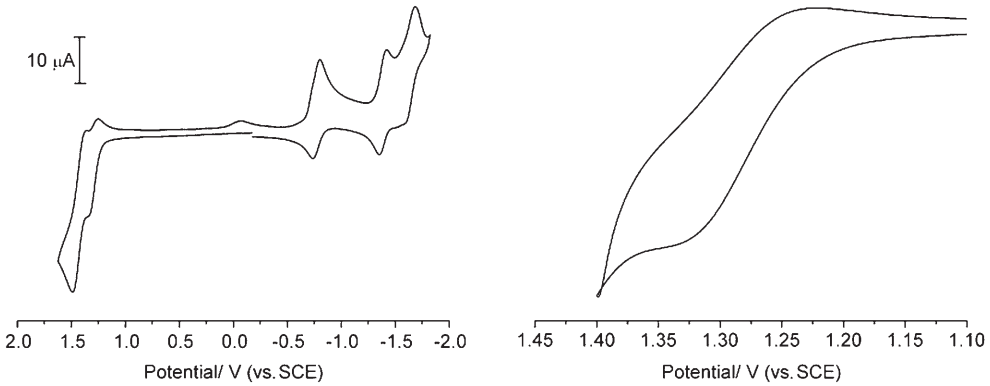

Figure 4. Cyclic voltammogram of **2d** in acetonitrile with 0.1 M $TBAPF_6$, with magnified view of the first oxidation process on the right.

the parent complex $[Ru(tpy)_2]^{2+}$ due to the ease of reducing the electron-deficient bis(pyridyl) triazine ligands relative to tpy.[13] The second reduction is tpy-based and compares well with the reduction of the parent complex $[Ru(tpy)_2]^{2+}$. The third reduction is assigned to a second one-electron reduction on the triazine ligand.

Homoleptic **3a** and **3b** have Ru^{III}/Ru^{II} couples at a more positive potential than the heteroleptic complexes as a result of the electron-deficient bis(pyridyl)triazine ligands drawing electron density away from the Ru^{II} metal centres. Anthracene-substituted **3d** has an additional oxidation consistent with an anthracene-based oxidation as in **2d**, also confirmed as irreversible as a result of the difference between its cathodic and anodic peak potentials and its I_c/I_a ratio.

Complexes **3** have several irreversible ligand-based reductions. There are two one-electron reductions on each triazine unit to give a total of four reductions. The separation between the second and third reduction processes is in the range 610–660 mV for all of the complexes (leaving aside **3e**, whose irreversible third process makes the comparison impossible), in good agreement with the electron-pairing energy in tpy-type ligands.[42]

Table 3. Spectroscopic and photophysical data of the complexes in solutions of deaerated acetonitrile (298 K) or in a butyronitrile rigid matrix (77 K).[24]

Compound	Absorption at 298 K	Luminescence at 298 K			Luminescence at 77 K	
	λ_{max} [nm] (ε [$M^{-1}cm^{-1}$])	λ_{max} [μm]	λ	τ [ns]	λ_{max} [nm]	τ [μs]
2a	282 (53.5); 301 (59.6) 476 (21.7)	739	1.2×10^{-4}	12	693	1.2
2b	273 (59.0); 301 (52.2) 332 (48.6); 478 (27.7)	733	1.0×10^{-4}	10	695	1.9
2c	254 (83.1); 273 (79.9) 299 (73.2); 331 (34.3) 477 (26.3)	734	0.9×10^{-4}	13	694	2.0
2d	254 (121.4); 282 (55.7) 299 (56.5); 364 (14.4) 383 (12.3); 477 (25.7)	735	1.0×10^{-4}	13	694	3400
2e	258 (59.3); 272 (35.7) 281 (36.1); 298 (34.6) 330 (sh); 357 (9.2) 377 (9.1); 397 (8.3) 478 (15.4)	738	0.5×10^{-4}	54	695	3400
3a	279 (50.9); 295 (50.6) 491 (27.5)	714	$<10^{-5}$	2	676	2.0
3b	276 (64.7); 339 (49.6) 501 (26.5)	–	–	–	682	2.2
3c	206 (86.1); 253 (85.6) 274 (74.7); 328 (sh) 491 (21.1)	717	$<10^{-5}$	6	678	2.2
3d	254 (145.1); 280 (46.7) 346 (16.4); 364 (14.9) 383 (12.9); 494 (20.7)	–	–	–	694	3500
3e	258 (155.6); 279 (60.7) 357 (15.6); 377 (18.2) 397 (17.3); 493 (26.8)	–	–	–	694	4200

Absorption spectra and photophysical properties: The electronic absorption and photophysical data of the new complexes are shown in Table 3. Representative absorption and emission spectra are shown in Figures 5–8. The absorption spectra are dominated by ligand-based spin-allowed $\pi\rightarrow\pi^*$ and $n\rightarrow\pi^*$ transitions in the UV region of the spectra and by ^{1}MLCT absorption bands in the visible region (Table 3, Figures 5 and 6). Complexes **2a–e** have a relatively sharp

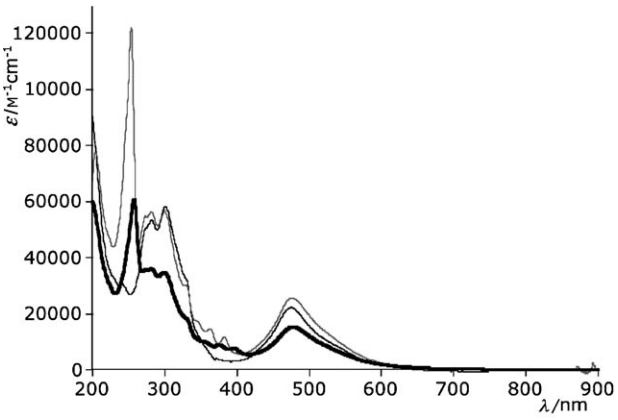

Figure 5. Absorption spectra of **2a** (straight line), **2d** (grey line) and **2e** (bold line).

^{1}MLCT absorption band, with the λ_{max} value corresponding to the transition involving the tpy ligand. A low-energy shoulder corresponds to the singlet MLCT transition involv-

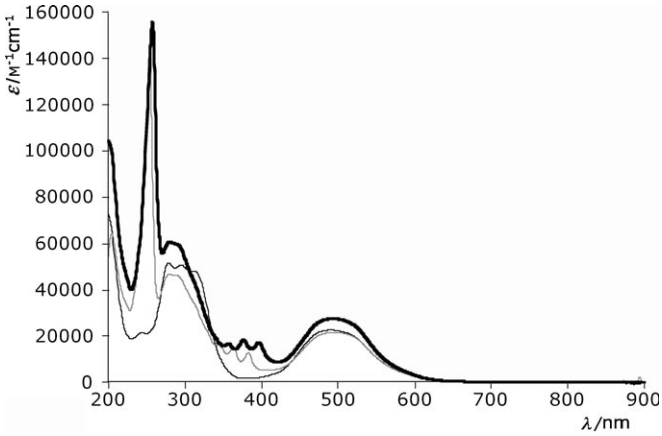

Figure 6. Absorption spectra of **3a** (straight line), **3d** (grey line) and **3e** (bold line).

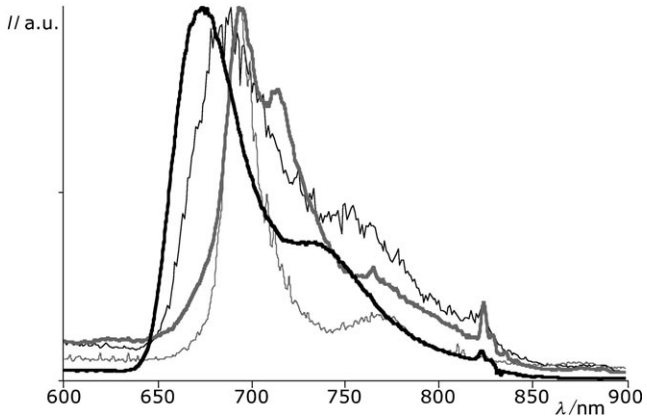

Figure 8. Uncorrected emission spectra of **2b** (straight line), **2d** (grey line), **2e** (bold grey line) and **3a** (bold line) in a butyronitrile rigid matrix at 77 K.

ing the bis(pyridyl)triazine ligands.[13] Complexes **2d** and **2e** have additional characteristic sharp high-energy transitions that correspond to the $\pi\rightarrow\pi^*$ transitions associated with the anthracene component (Figure 5).[43,44] The same absorption features are observed in the homoleptic complexes **3d** and **3e**. The ^{1}MLCT bands in the homoleptic complexes are broader, and the visible maxima are red-shifted relative to the spectra of **2a**-**-e**, as a consequence of missing the higher-energy MLCT transitions involving the tpy ligand.[13]

The room-temperature emission of the heteroleptic complexes **2a**–**e** can be assigned to triplet MLCT states involving the bis(pyridyl)triazine ligands on the basis of the energies and shapes (Table 3 and Figures 7 and 8).[13] As far as the homoleptic **3a**–**e** species are concerned, only **3a** and **3c** exhibit a sizeable room-temperature emission, assigned to the lowest-lying MLCT triplet state, whereas **3b**, **3d** and **3e** do not emit at room temperature. This behaviour is probably due to the lowering of the energy of the metal-centred (MC) state, as a consequence of increased distortion in the octahedral geometry exhibited by the homoleptic compounds relative to the heteroleptic species, as supported by the comparison of crystallographic data of **2a** and **3a.** Such a lowering of the MC state makes this latter level closer in energy to the MLCT state, so thermally activated surface crossing to the MC state is very efficient and finally leads to very fast radiationless decay, which prevents luminescence.

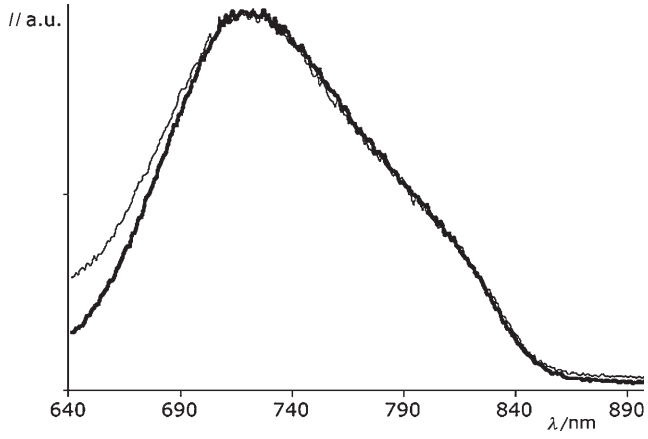

Figure 7. Uncorrected emission spectra of **2a** (bold line) and **2e** (straight line) in solution with acetonitrile at room temperature. See Table 3 for the corrected maxima values.

In the whole series of complexes, varying the substituent at the *para* position of the phenyl ring has little effect on the energy of the MLCT absorption and emission bands, thus indicating that the aryl groups are largely electronically separated from the Ru^{II} centre and the associated MLCT states. However, the excited-state lifetimes are influenced to a greater extent; in fact, whereas **2a**–**d** have excited-state lifetimes between 10 and 13 ns, approximately fifty-times longer lived than the parent complex $[Ru(tpy)_2]^{2+}$ at room temperature and well comparable with those of other Ru^{II}–triazine-based compounds,[13] the excited-state lifetime of **2e** is significantly longer (Table 3). Indeed, hydrocarbon aromatic chromophores appended to metal complexes can prolong MLCT emission lifetimes.[16,17] However, biphenyl, phenanthryl and anthryl groups, which are present in **2b, 2c** and **2d**, respectively, have no sizeable effect on the MLCT lifetime at room temperature. The reason is that the lowest-energy MLCT state in these complexes is so low lying that thermal population of the relevant aromatic organic triplets (whose lowest-energy triplet is that of the 9-aryl anthracene chromophore, at about 685 nm[16,42,43]) is ineffective; furthermore, the intrinsic decay rates of aromatic hydrocarbons and MLCT triplets should be taken into consideration. As far as **2e** is concerned, this species bears a brominated anthracene and the electron-withdrawing effect of the bromo substituent lowers the energy of the anthracene-based triplet state. Actually, comparison between the triplet state of anthracene ($14\,870\ cm^{-1}$)[43,45] and 9-bromoanthracene ($14\,400\ cm^{-1}$)[44,46] suggests that a bromo substituent stabilises the anthracene-based triplet state by about $500\ cm^{-1}$. Assuming the same effect in the present systems and considering that the triplet state of the aryl anthracene/Ru^{II} complexes is at about 685 nm (see above), as also evidenced by

the low-temperature emission of similar complexes,[16] the triplet state of the bromoanthryl subunit in **2e** should lie at about 705 nm at room temperature. As a consequence, the lowest-energy triplet state of the aromatic anthryl-based chromophore in **2e** becomes low enough to make equilibration between the MLCT and anthryl-based triplets effective so that the multichromophoric effect can take place.

On cooling the samples to 77 K in a butyronitrile rigid matrix, the excited-state lifetimes of **2a–e**, as expected, are prolonged relative to room temperature. This effect is much larger for **2d** and **2e**, whose luminescence lifetimes under these conditions are three orders of magnitude longer than those of **2a–c** (Table 3). The shape of the emission is also different for **2d** and **2e** (in particular for the **2d** species, for which the higher-energy band is quite narrow) relative to those of **2a–c** (Figure 8). The lifetime and shape of the emissions clearly indicate that emission of **2a–c** are still from MLCT states, whereas for **2d** and **2e** emission has to be assigned to phosphorescence from the anthracene-based triplet states. In fact, CT states are destabilized on passing from a fluid solution at room temperature to a rigid matrix at 77 K,[3,47,48] whereas the energy of the organic triplets is essentially unperturbed by media conditions. Since the MLCT and anthryl-based triplet states are relatively close to one another in **2d** and **2e**, the energy order of the two states is inverted on passing to 77 K, an already reported behaviour for Ru^{II} complexes that contain anthracene derivatives.[49]

The emissions of **2d** and **2e** at 77 K both maximize at 695 nm. Surprisingly, **2d** and **2e** have the same emission maximum in this condition, thus suggesting that the presence of the bromo substituent is less important in the rigid matrix, as opposed to what happens at room temperature (see above). Indeed, it was expected that the emission energy of **2e** would be slightly lower than that of **2d**. We have no simple explanation for this behaviour, we could only infer that some intermolecular interactions involving the bromine atoms, as evidenced in the solid state of **3a** (see the X-ray crystallography section), can also occur in the rigid matrix for **2e** (and **3e**), thus making the presence of the bromo substituent on the anthracene unit less effective.

As far as the homoleptic complexes **3a–e** are concerned, all exhibit long-lived luminescence at 77 K, similar to the behaviour of their heteroleptic counterparts (Table 3). The same line of reasoning used for the emission of **2a–e** at 77 K allows us to assign the emission of **3a–c** to MLCT states and the emission of **3d** and **3e** to anthracene-based phosphorescence. Thermal population of the upper-lying MC states is not effective at 77 K, thus allowing luminescence from the homoleptic species. Interestingly, whereas the emission energies of **3d** and **3e** are identical to those of **2d** and **2e**, thus confirming their common anthryl-based origin and the constant energy level of the relevant aromatic hydrocarbon on passing from hetero- to homoleptic compounds, the emission energies of **3a–c** are slightly higher than those of the corresponding **2a–c** species, in agreement with the redox potentials and supporting once more their MLCT origin.

Conclusion

We prepared a series of new hetero- and homoleptic Ru^{II} complexes based on bis(pyridyl)triazine ligands and studied their absorption spectra, redox behaviour and luminescence properties, both at room temperature in fluid solution and at 77 K in a rigid matrix. In some complexes, the anthryl groups are linked to the triazine-based ligands.

The excited-state lifetimes of the heteroleptic complexes **2a–e** are significantly longer than that of the parent complex $[Ru(tpy)_2]^{2+}$ and the homoleptic triazine complexes **3a–e** at room temperature. The presence of the triazine ligand lowers the energy of the ligand-based orbitals and, therefore, the MLCT states, whilst the metal-centred states are maintained at higher energy in **2a–e** by the presence of an orthogonal tpy ligand. In homoleptic triazine complexes **3a–e**, the MC states are lower in energy as a result of the small tridentate N-M-N bite angle, as observed in the solid state. As a consequence, a minimal improvement is observed in the excited-state properties of **3a–e** relative to the parent complex $[Ru(tpy)_2]^{2+}$.

The introduction of additional chromophores can have an impact on the excited-state lifetime when the energy of the organic component is comparable to the energy of the ^{3}MLCT state. This result is obtained by tuning the excited-state energy of the anthracene subunit with the introduction of a bromo substituent. The lowering in energy of the ^{3}bromoanthracene excited state, which can then interact with the emissive ^{3}MLCT state in **2e**, extends the excited-state lifetime to 54 ns at room temperature as compared to an excited-state lifetime of 13 ns for **2d**, which bears an unsubstituted anthracene unit. The use of stronger electron-withdrawing (cyano) and electron-delocalising (acetylene) groups to further tune the excited-state energy of the anthryl chromophore, and therefore the MLCT luminescence lifetime, will be investigated in due course.[50]

Acknowledgements

The authors thank the Natural Sciences and Engineering Research Council of Canada, Université de Montréal, the Centre for Self-Assembled Chemical Systems, and the University of Messina for financial support, the ICCS for funding (E.A.M.), F. Bélanger-Gariépy for assistance with the X-ray analysis and Johnson Matthey plc for a loan of $[RuCl_3]\cdot 3H_2O$.

[1] V. Balzani, A. Juris, M. Venturi, S. Campagna, S. Serroni, *Chem. Rev.* **1996**, *96*, 759.
[2] K. Kalyanasundaram, *Photochemistry of Polypyridine and Porphyrin Complexes*, 1st ed., Academic Press, San Diego, **1992**.
[3] A. Juris, V. Balzani, F. Barigelletti, S. Campagna, P. Belser, A. Von Zelewsky, *Coord. Chem. Rev.* **1988**, *84*, 85.
[4] V. Balzani, S. Campagna, G. Denti, A. Juris, S. Serroni, M. Venturi, *Acc. Chem. Res.* **1998**, *31*, 26.
[5] J. K. McCusker, *Acc. Chem. Res.* **2003**, *36*, 876.
[6] T. J. Rutherford, D. A. Reitsma, F. R. Keene, *J. Chem. Soc. Dalton Trans.* **1994**, 3659.

[7] J. P. Sauvage, J. P. Collin, J. C. Chambron, S. Guillerez, C. Coudret, V. Balzani, F. Barigelletti, L. De Cola, L. Flamigni, *Chem. Rev.* **1994**, *94*, 993.
[8] M. Abrahamsson, M. Jaeger, T. Oesterman, L. Eriksson, P. Persson, H.-C. Becker, O. Johansson, L. Hammarstroem, *J. Am. Chem. Soc.* 2006, 128, 12616.
[9] J. R. Winkler, T. L. Netzel, C. Creutz, N. Sutin, *J. Am. Chem. Soc.* **1987**, *109*, 2381.
[10] E. A. Medlycott, G. S. Hanan, *Chem. Soc. Rev.* **2005**, *34*, 133.
[11] E. A. Medlycott, G. S. Hanan, *Coord. Chem. Rev.* **2006**, *250*, 1763.
[12] M. I. J. Polson, N. J. Taylor, G. S. Hanan, *Chem. Commun.* **2002**, 1356.
[13] M. I. J. Polson, E. A. Medlycott, G. S. Hanan, L. Mikelsons, N. J. Taylor, M. Watanabe, Y. Tanaka, F. Loiseau, R. Passalacqua, S. Campagna, *Chem. Eur. J.* **2004**, *10*, 3640.
[14] N. D. McClenaghan, Y. Leydet, B. Maubert, M. T. Indelli, S. Campagna, *Coord. Chem. Rev.* **2005**, *249*, 1336.
[15] a) W. E. Ford, M. A. J. Rodgers, *J. Phys. Chem.* **1992**, *96*, 2917; b) G. J. Wilson, A. Launikonis, W. H. F. Sasse, A. W.-H. Mau, *J. Phys. Chem. A* **1997**, *101*, 4860; c) J. A. Simon, S. L. Curry, R. H. Schmehl, T. R. Schatz, P. Piotrowiak, X. Jin, R. P. Thummel, *J. Am. Chem. Soc.* **1997**, *119*, 11012; d) A. Harriman, M. Hissler, A. Khatyr, R. Ziessel, *Chem. Eur. J.* **1999**, *5*, 3366; e) D. S. Tyson, C. R. Luman, X. Zhou, F. N. Castellano, *Inorg. Chem.* **2001**, *40*, 4063; f) N. D. McClenaghan, F. Barigelletti, B. Maubert, S. Campagna, *Chem. Commun.* **2002**, 6, 602; g) S. Leroy-Lhez, C. Belin, A. D′Aleo, R. Williams, L. De Cola, F. Fages, *Supramol. Chem.* **2003**, *15*, 627; h) X. Y. Wang, A. Del Guerzo, R. H. Schmehl, *J. Photochem. Photobiol. C* **2004**, *5*, 55; i) J. Wang, Y.-Q. Fang, G. S. Hanan, F. Loiseau, S. Campagna, *Inorg. Chem.* **2005**, *44*, 5.
[16] a) R. Passalacqua, F. Loiseau, S. Campagna, Y.-Q. Fang, G. S. Hanan, *Angew. Chem.* **2003**, *115*, 1646; *Angew. Chem. Int. Ed.* **2003**, *42*, 1608; b) J. Wang, Y.-Q. Fang, L. Bourget-Merle, M. I. J. Polson, G. S. Hanan, A. Juris, F. Loiseau, S. Campagna, *Chem. Eur. J.* **2006**, *12*, 8539.
[17] B. Maubert, N. D. McClenaghan, M. T. Indelli, S. Campagna, *J. Phys. Chem. A* **2003**, *107*, 447.
[18] Strictly speaking, the states involved in the equilibration process can be much more than two; in Ru^{II}– polypyridine complexes, such as $[Ru(bpy)_3]^{2+}$, for example, the lowest-energy ^{3}MLCT manifold is made of three closely spaced levels.[3,46] However, these levels are equilibrated at room temperature and 77 K and can be considered as a "single" state.
[19] C. J. Aspley, J. A. G. Williams, *New J. Chem.* **2001**, *25*, 1136.
[20] C. Patoux, J.-P. Launay, M. Beley, S. Chodorowski-Kimmes, J.-P. Collin, S. James, J.-P. Sauvage, *J. Am. Chem. Soc.* **1998**, *120*, 3717.
[21] S. J. Dunne, E. C. Constable, *Inorg. Chem. Commun.* **1998**, *1*, 167.
[22] E. C. Constable, A. M. W. Cargill Thompson, S. Greulich, *J. Chem. Soc. Chem. Commun.* **1993**, 1444.
[23] M. Beley, J. P. Collin, R. Louis, B. Metz, J. P. Sauvage, *J. Am. Chem. Soc.* **1991**, *113*, 8521.
[24] Emission quantum yields were measured at room temperature using the optically dilute methods, see: G. A. Crosby, J. N. Demas, *J. Phys. Chem.* **1971**, *75*, 991. $[Ru(bpy)_3]^{2+}$ in air-equilibrated aqueous solution and $[\{(bpy)_2Ru(\mu\text{-}2,3\text{-}dpp)\}_3Ru]^{8+}$ (2,3-dpp = 2,3-bis(2′-pyridyl)-pyrazine) in deaerated acetonitrile solution were used as quantum yield standards, assuming values of 0.028[25] and 0.005,[26] respectively.
[25] N. Nakamaru, *Bull. Chem. Soc. Jpn.* **1982**, *55*, 2697.
[26] S. Campagna, G. Denti, S. Serroni, A. Juris, M. Venturi, V. Ricevuto, V. Balzani, *Chem. Eur. J.* **1995**, *1*, 211.
[27] E. A. Medlycott, I. Theobald, G. S. Hanan, *Eur. J. Inorg. Chem.* **2005**, 1223.
[28] B. P. Sullivan, J. M. Calvert, T. J. Meyer, *Inorg. Chem.* **1980**, *19*, 1404.
[29] M. Baumgarten, L. Gherghel, J. Friedrich, M. Jurczok, W. Rettig, *J. Phys. Chem. A* **2000**, *104*, 1130.
[30] S. Kotha, A. K. Ghosh, K. D. Deodhar, *Synthesis* **2004**, *4*, 594.
[31] E. A. Medlycott, G. S. Hanan, *Inorg. Chem. Commun.* **2006**, DOI: 10.1016/j.inoche.2006.10.023.
[32] K. O. Johansson, J. A. Lotoski, C. C. Tong, G. S. Hanan, *Chem. Commun.* **2000**, 819.
[33] F. Loiseau, R. Passalacqua, S. Campagna, M. I. J. Polson, Y.-Q. Fang, G. S. Hanan, *Photochem. Photobiol. Sci.* **2002**, *1*, 982.
[34] K. J. Arm, J. A. G. Williams, *Chem. Commun.* **2005**, 230.
[35] K. J. Arm, J. A. G. Williams, *Dalton Trans.* **2006**, 2172.
[36] G. J. Pernìa, J. D. Kilburn, J. W. Essex, R. J. Mortishire-Smith, M. Rowley, *J. Am. Chem. Soc.* **1996**, *118*, 10220.
[37] N. W. Alcock, P. R. Barker, J. M. Haider, M. J. Hannon, C. L. Painting, Z. Pikramenou, E. A. Plummer, K. Rissanen, P. Saarenketo, *Dalton Trans.* **2000**, 1447.
[38] S. Pyo, E. Perez-Cordero, S. G. Bott, L. Echegoyen, *Inorg. Chem.* **1999**, *38*, 3337.
[39] E. A. Medlycott, K. A. Udachin, G. S. Hanan, *Dalton Trans.* **2007**, in press.
[40] A. Harriman, A. Mayeux, A. De Nicola, R. Ziessel, M. Beley, *Phys. Chem. Chem. Phys.* **2002**, *4*, 2229.
[41] Although a theoretical value of 59 mV is expected for the difference between the cathodic and anodic waves for a reversible one-electron process, small deviations from this value have previously been reported as "reversible"; see, for example: reference [26] and A. Harriman, M. Hissler, A. Khatyr, R. Ziessel, *Chem. Eur. J.* **1999**, *5*, 3366, and references therein. We thank a reviewer for suggesting the inclusion of I_c/I_a ratios to Table 2 as another measure of the irreversibility of the processes described therein.
[42] A. Mamo, I. Stefio, M. F. Parisi, A. Credi, M. Venturi, C. Di Pietro, S. Campagna, *Inorg. Chem.* **1997**, *36*, 5947.
[43] S. L. Murov, I. Carmichael, G. L. Hug, in *Handbook of Photochemistry*, Marcel Dekker, New York, **1993**.
[44] *Handbook of Photochemistry, 3rd Edition, Revised and Expanded* (Eds.: M. Montalti, A. Credi, L. Prodi, M. T. Gandolfi), CRC Press, **2006**.
[45] D. F. Evans, *J. Chem. Soc.* **1957**, 1351.
[46] K. Hamanoue, S. Tai, T. Hikada, T. Nakayama, M. Kimoto, H. Teranashi, *J. Phys. Chem.* **1984**, *88*.
[47] T. J. Meyer, *Pure Appl. Chem.* **1986**, *58*, 1193, and references therein.
[48] P. Chen, T. J. Meyer, *Chem. Rev.* **1998**, *98*, 1439.
[49] a) S. Serroni, S. Campagna, R. Pistone Nascone, G. S. Hanan, G. J. Davidson, J.-M. Lehn, *Chem. Eur. J.* **1999**, *5*, 3523; b) J. Wang, E. A. Medlycott, G. S. Hanan, F. Loiseau, S. Campagna, *Inorg. Chim. Acta*, **2006**, in press.
[50] CCDC-619166–619169 contain the supplementary crystallographic data. These data can be obtained free of charge from The Cambridge Crystallographic Data Centre via www.ccdc.cam.ac.uk/data request/cif.

Received: September 25, 2006
Published online: December 21, 2006

